

Abstract

Electrospinning is a polymeric fiber production technique that is currently being researched for various applications, including membranes and filters, solar cells and fuels cells, tissue engineering and drug delivery. Several models have been developed that depict the mechanics behind electrospinning jets. Many of these models incorporate key principles in their analysis, such as conservation of charge and conservation of momentum, to predict electrospinning behavior. However, these current models disregard the role of heat and mass transfer and tend to assume operating parameters that do not represent typical electrospinning conditions. The objective of this project is to build upon current electrospinning models to include heat and mass transfer principles, environment conditions and realistic electrospinning operating parameters. Furthermore, the goal of the project is to identify the key dimensional parameters that have a significant affect to the control and operation of the electrospinning process. To validate the model, electrospinning and electro spraying experiments were ran for various solutions. The solutions tested include 4 wt% PEO/H₂O, 12 wt% PVP/BuOH, methanol, and butanol for injection rates ranging between 0.04 mL/min to 0.30 mL/min. At various injection rates, the supply voltage and current from the grounded plate were noted for further dimensionless analysis. Additionally, thermal imaging was utilized for several data sets to highlight the role of heat transfer between the polymeric jet and environment. Also, a microscope digital camera was utilized to capture images of the Taylor cone shape under different operating conditions.

Background

Electrospinning has five stages: 1) Charging of the polymeric solution 2) Formation of a Taylor cone and jet 3) Jet thins/stretch in presence of an electric field 4) Solvent evaporates 5) Collection of the fibers. There are many factors that play a role in electrospinning, including the solution properties, applied voltage, working distance, percent relative humidity, and spinning time.

The current slender jet model incorporates conservation of momentum and charge principles, as well as coulomb's law. The updated model takes into account mass balance, mass transfer, and an energy balance.

$$\begin{aligned} \text{Mass balance} & \sum_i \dot{m}_i' = R^2 u \\ \text{Charge balance} & R^2 E + \rho_e R u \sigma = 1 \\ \text{Coulomb's Law} & E = E_\infty - \left[(\sigma R)' - \frac{\rho}{2} (ER^2)' \right] \ln(x) \\ \text{Momentum balance} & \frac{(R^2 u^2)'}{R^2} = \frac{1}{Fr} + \frac{3(R^2 u)'}{Re R^2} + \frac{(R^2 \kappa)'}{We R^2} + \Lambda \left(\sigma \sigma' + \beta E E' + \frac{2\sigma E'}{R} \right) \\ \text{Mass transfer} & (u)' = -2(Ru)' S \frac{c'}{c} + \frac{D}{R^2} (c^2)' \\ \text{Energy balance} & \left[\sum_i \dot{m}_i' \theta_i' \right] - \frac{1}{G} \left[\rho R^2 \right]' = 2(Ru)' S (\theta - \theta_\infty) + \sum_i \frac{1}{\rho_i} (u^2)' \end{aligned}$$

Characteristic Scales

$$\begin{aligned} R &= \frac{R}{R_0} \\ \chi &= \frac{L}{R_0} \\ \theta &= \frac{T}{T_0} \\ n_0 &= \frac{\rho_0 \rho_e'}{M_0^2} \\ E_0 &= \frac{I}{\pi R_0^2 K} \end{aligned}$$

Dimensionless Groups

$$\begin{aligned} Fr &= \frac{u_0^2}{g R_0} & We &= \frac{\rho_e u_0^2 R_0}{\gamma} & Ca &= \frac{W_e}{Re} \\ Re &= \frac{u_0 \rho_e R_0}{\eta_0} & Pe_e &= \frac{2 \tilde{E} u_0}{K R_0} & \Lambda &= \frac{\tilde{E} E_0^2}{\rho_e u_0^2} \\ Re_g &= \frac{u_0 \rho_e R_0}{\eta_0} & Sc' &= \frac{v}{D'} \end{aligned}$$

Objective

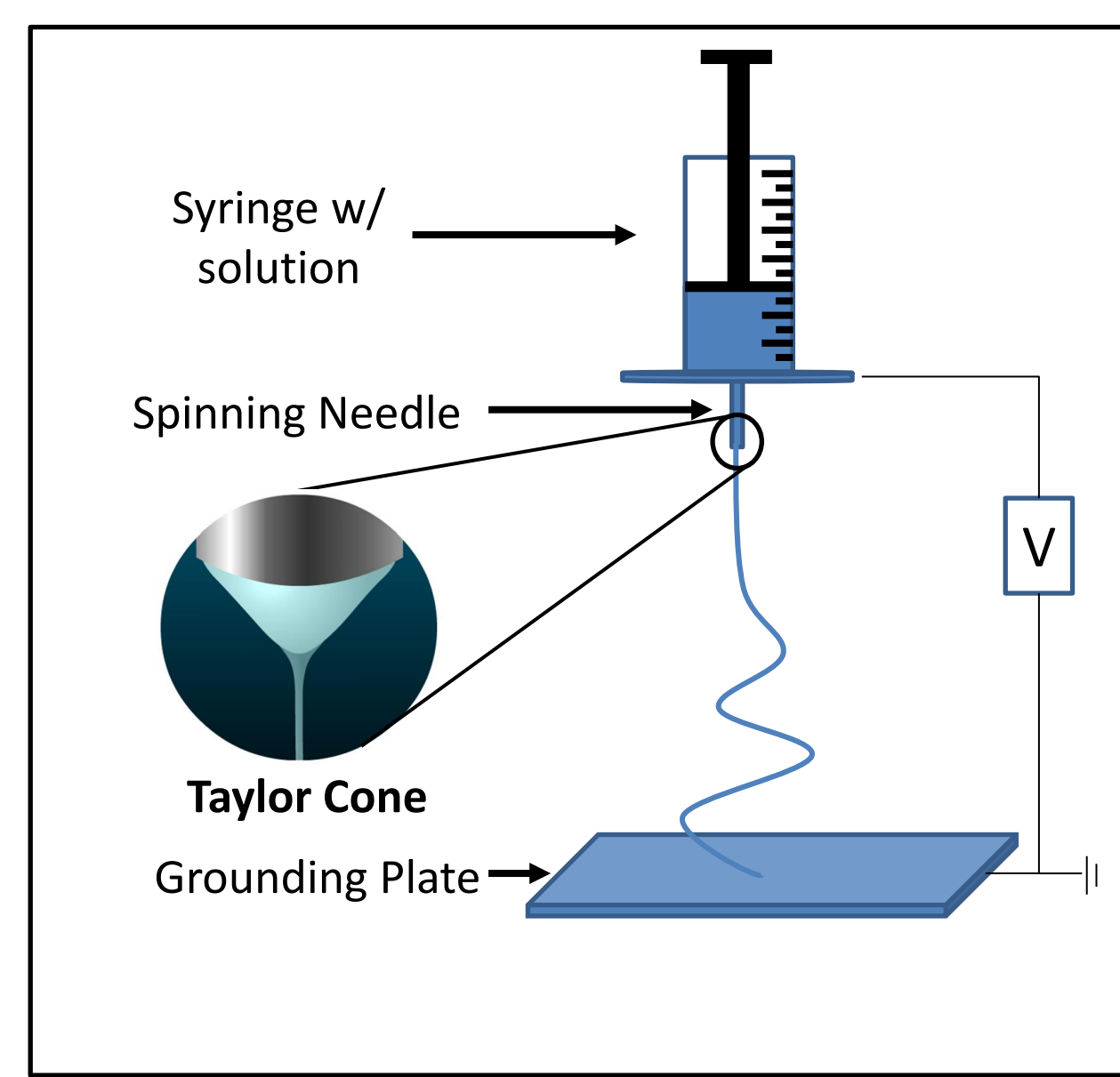
To build upon current slender jet models to include the role of heat and mass transfer and environment conditions. Furthermore, to identify key dimensionless parameters that have a significant affect to the control and operation of the electrospinning process.

Materials & Methods

The following solutions were first prepared:

- 4 wt% PEO/H₂O
- 12 wt% PVP/BuOH
- Methanol
- Butanol

After solution preparation, a solution was filled into a syringe, placed onto the PHD 2000 Infusion, and a desired infusion rate was chosen. Once dripping was observed at the spinning needle, a supply voltage between 10 to 20 kV was applied to the electrospinning plate. The voltage was adjusted accordingly until the jet formed a steady Taylor cone. Once steady-state was achieved, optical images were taken to observe the jet profile as well as thermal images to observe the heat transfer between the jet and environment. Additionally, the voltage drop across a 200 kΩ resistor in series with the grounded wire was measured using a Fluke multimeter, which was then used to calculate current using Ohms law. The solution type, infusion rate, supplied voltage, current, working distance, and percent relative humidity were all recorded. The data was then used to determine dimensionless groups of interest and inputted into a model that simulates the electrospinning behavior. Experimental images and the simulation's model were ultimately compared.



Schematic of Conventional Electrospinning Setup

Results

The effect of increasing the supply voltage on the jet profile and dimensionless values (Pe/Λ & Ca) can be observed in the following table. Additionally, Pictures 1 to 3 show the actual image of the jet profile, the simulated jet profile, and the two images overlapped for comparison (left to right).

Table 1. Jet profile images and dimensionless values at different conditions for 12 wt% PVP/BuOH solution

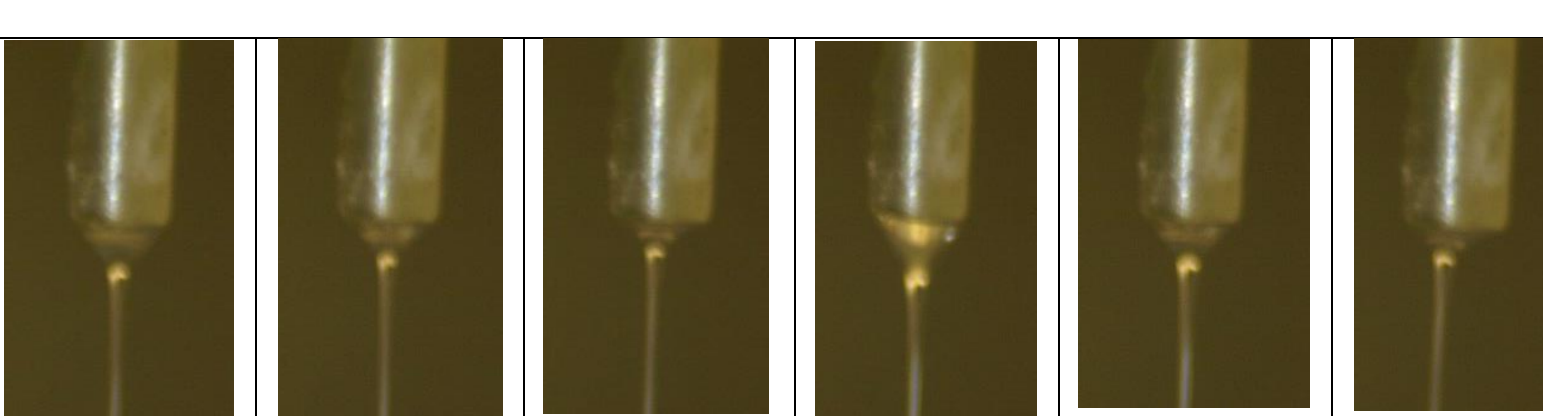
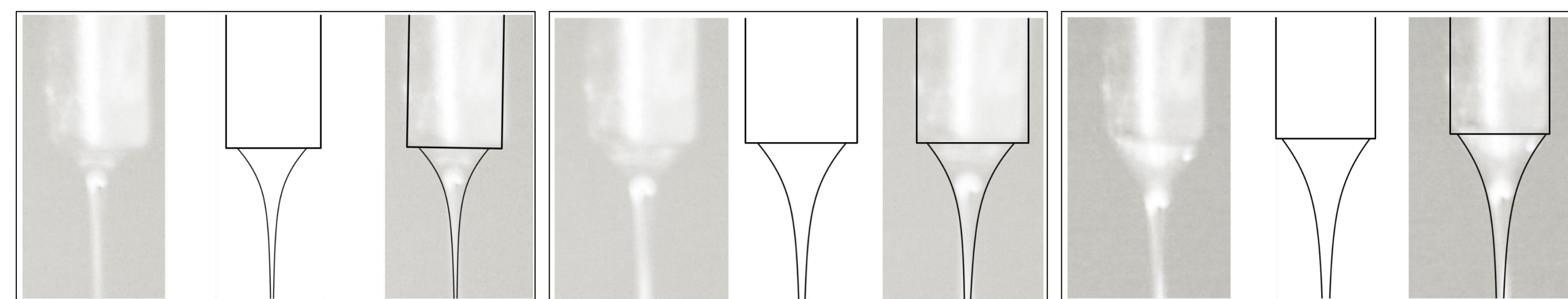
12 wt% PVP/BuOH Taylor Cone Images:						
Infusion Rate (mL/min)	0.07	0.07	0.07	0.09	0.09	0.09
Supply Voltage (kV)	11.6	12	12.8	11.2	12.0	13.4
Pe/Λ	7.95E+03	9.27E+03	1.04E+04	4.00E+03	4.96E+03	6.96E+03
Ca	15.7	15.7	15.7	12.2	12.2	12.2

Table 2. Comparison of actual Pe/Λ & Ca values versus simulated

Picture	Pe/Λ	Ca
	Actual	
1	1.04E+04	21.9
2	4.96E+03	12.2
3	4.00E+03	12.2
Simulated		
1	1.04E+04	18.9
2	4.94E+04	12.6
3	4.00E+03	13.6



Picture 1

Picture 2

Picture 3

Results

Figures 1 and 2 are plots of the momentum balance and coulomb's law for the simulated data for the Ca = 13.6 and Pe/Λ = 4000. Figure 1 shows which terms contribute to the forces on the jet at some dimensionless distance. Positive dimensionless momentum is an attractive (or stretching force) and a negative dimensionless momentum is a resistance to stretching force.

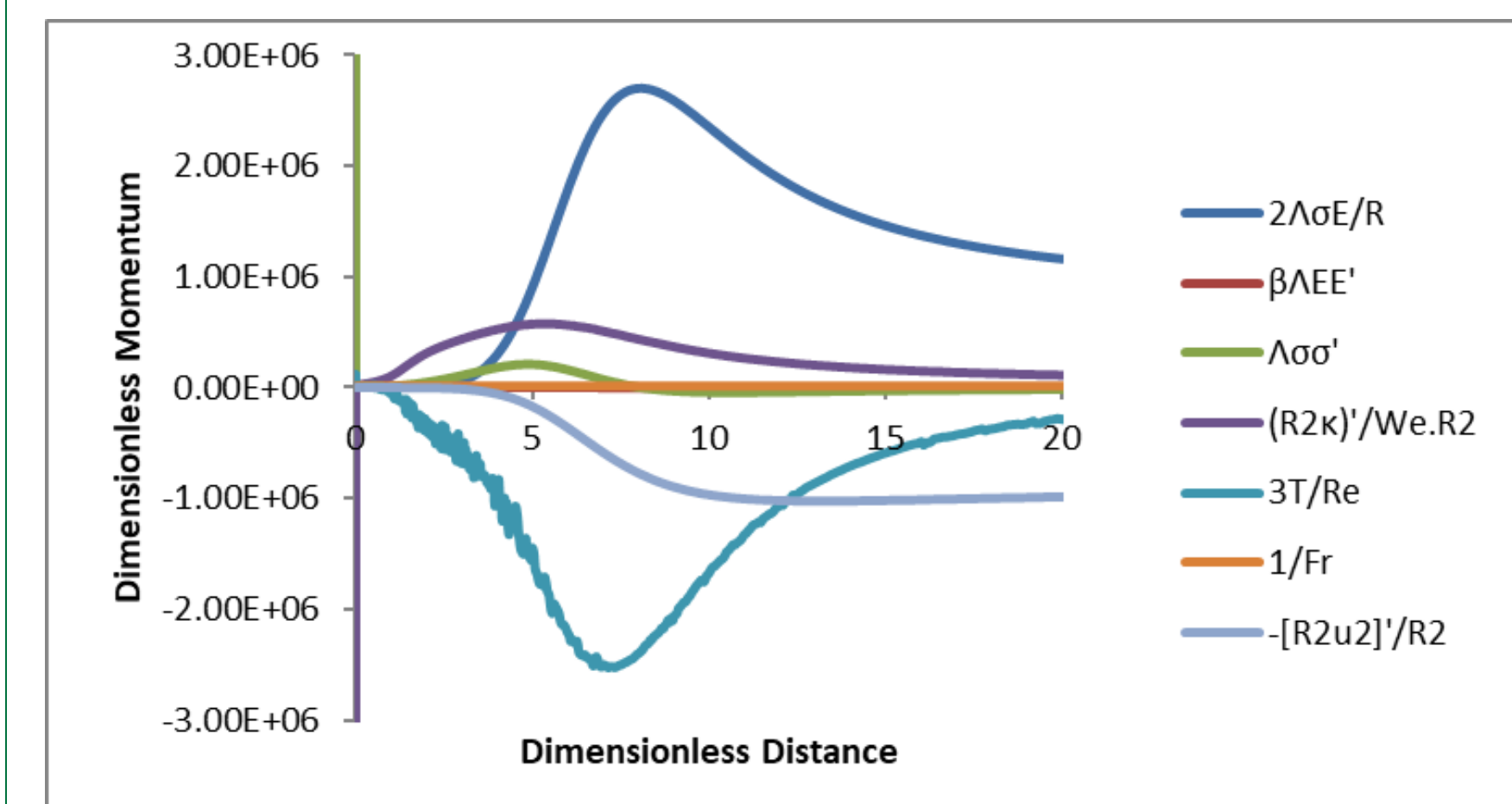


Figure 1. Dimensionless momentum versus dimensionless distance

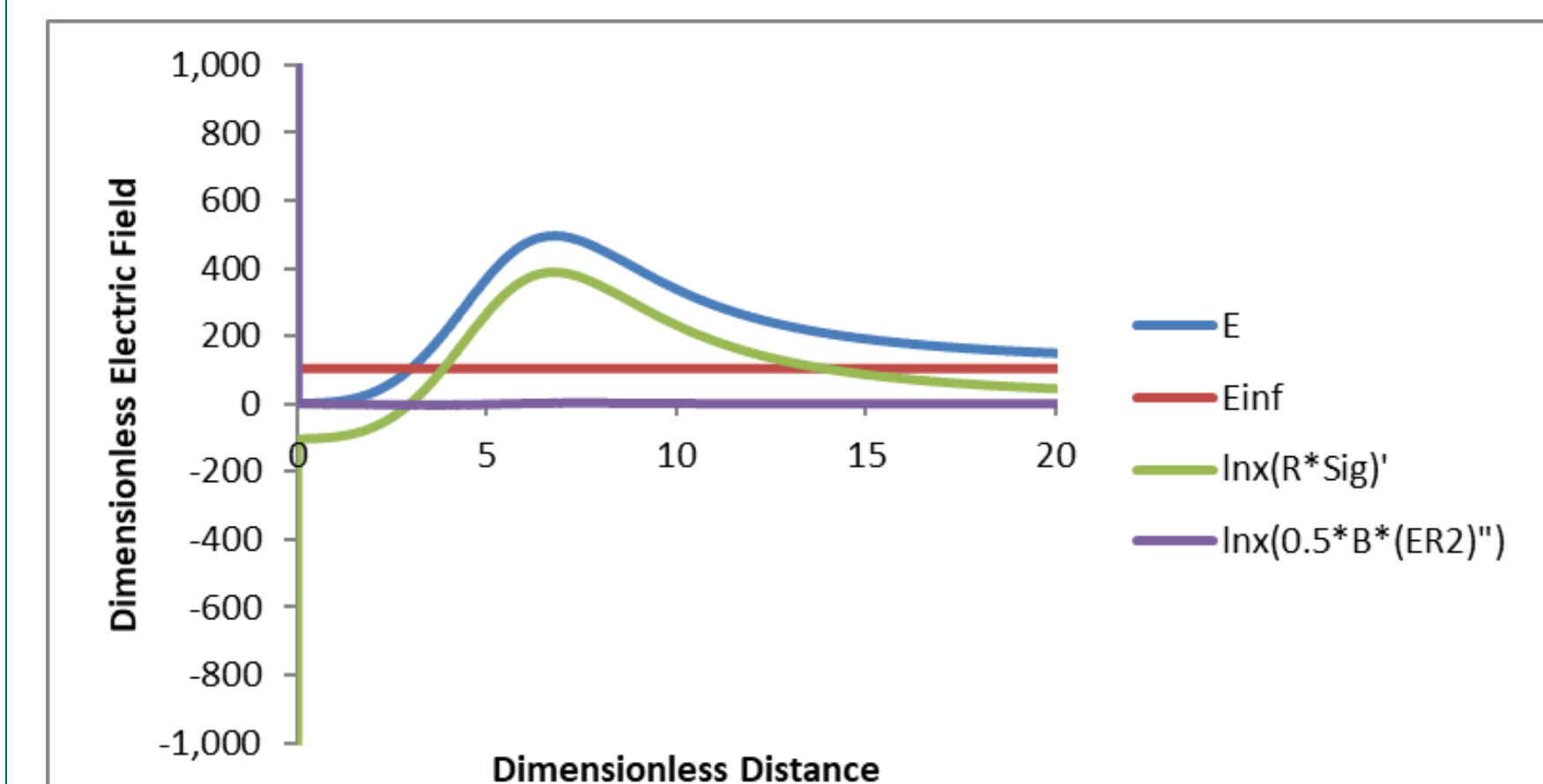


Figure 2. Dimensionless electric field versus dimensionless distance

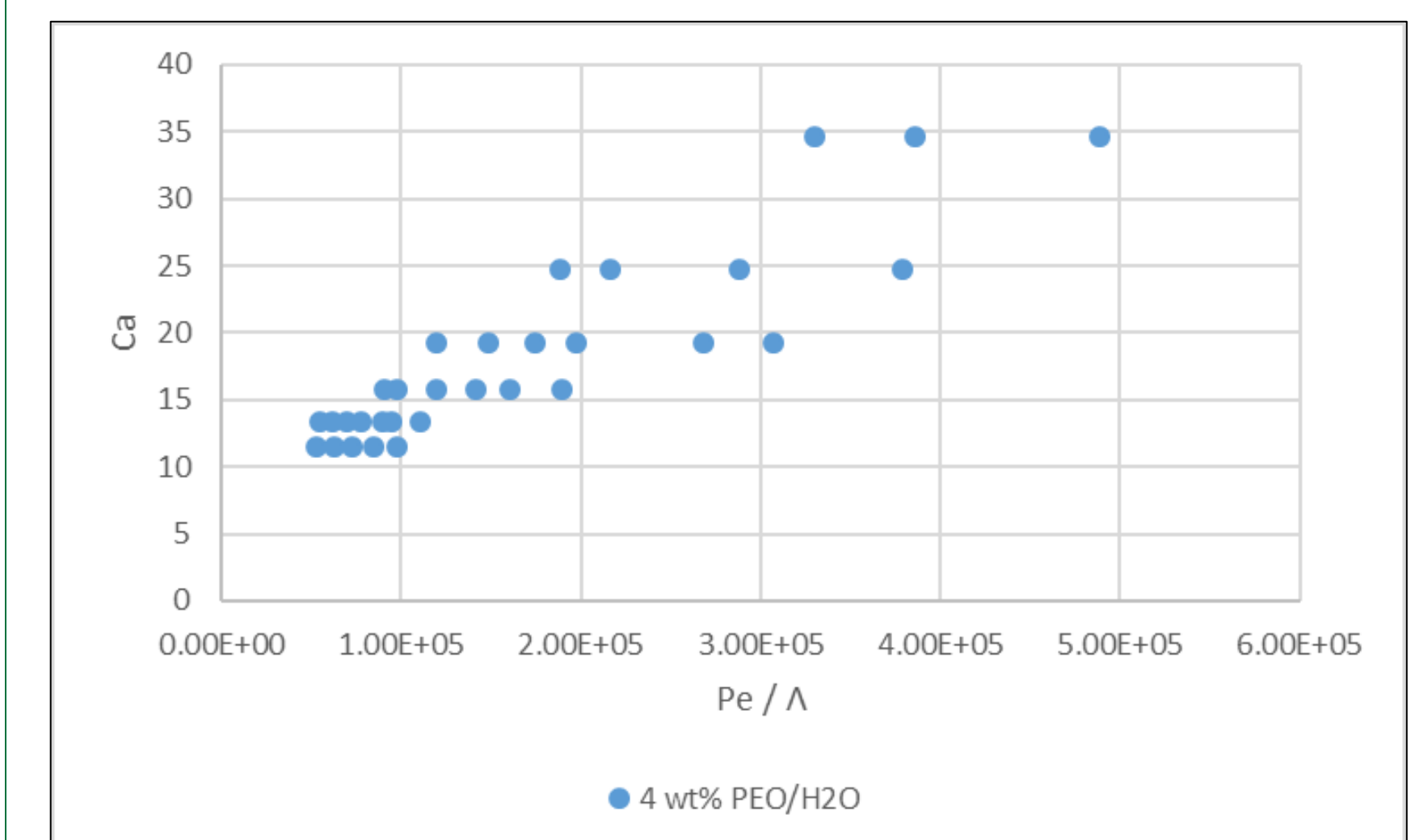


Figure 3. Ca versus Pe/Λ for 4wt% PEO/H₂O

Conclusion

Summary

- Developed and tested a model to include mass transfer, heat transfer, and environmental conditions
- Compared simulated jet profiles and dimensionless groups to experimental results

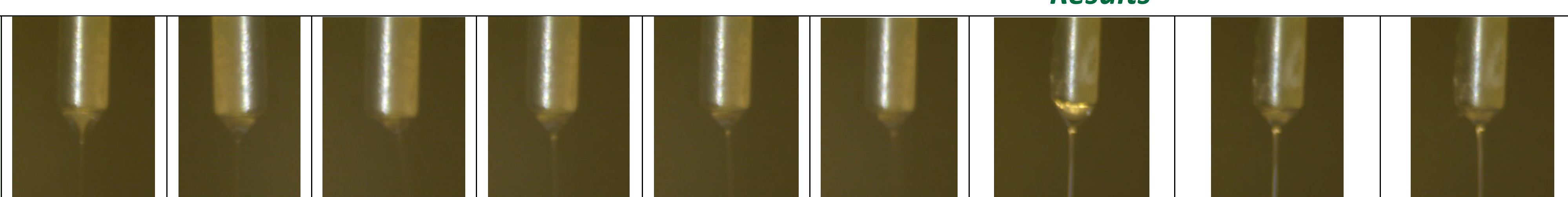
Future Work

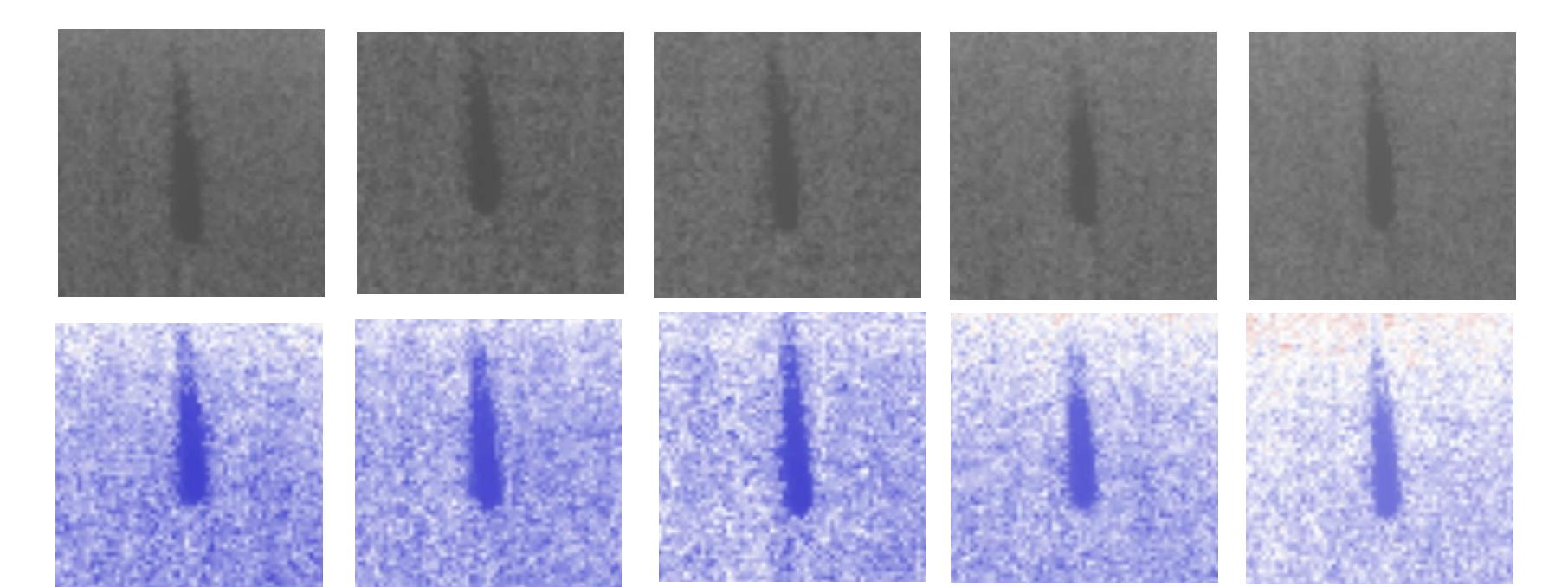
- Continue to refine model and gather experimental data to verify simulation results
- Electrospin more solutions

Acknowledgement

I would like to thank my faculty advisor, Dr. Keith Forward, for his support and encouragement during this project.

Results

Jet Profile Images										
Solution	BuOH	BuOH	BuOH	BuOH	BuOH	BuOH	12 wt% PVP/BuOH	12 wt% PVP/BuOH	12 wt% PVP/BuOH	
Infusion Rate (mL/min)	0.05	0.05	0.05	0.15	0.15	0.15	0.05	0.05	0.05	
Supply Voltage (kV)	17.3	18.3	19.1	18.6	19.0	19.6	11	11.3	11.6	



Thermal images of ethanol showing heat transfer between jet and environment; Inf Rate = 0.01 mL/min, V = 11.5 - 12.5 kV